

## Prestressing for Reduction of Local Vibrations in a Rotorcraft

Grzegorz SUWAŁA<sup>1)</sup>, Lech KNAP<sup>2)</sup>, Jan HOLNICKI-SZULC<sup>1)</sup>

<sup>1)</sup> *Institute of Fundamental Technological Research  
Polish Academy of Sciences*

Pawińskiego 5B, 02-106 Warszawa, Poland  
e-mail: {gsuwala, holnicki}@ippt.pan.pl

<sup>2)</sup> *Institute of Vehicles*

*Faculty of Automotive and Construction Machinery Engineering  
Warsaw University of Technology  
Narbutta 84, 02-524 Warszawa, Poland*

The main objective of this paper is to investigate the possibility of local structural vibration suppression via introducing initial prestressing. In order to evaluate the effectiveness of the proposed method, a two-step approach has been used. Firstly, a prestressed modal analysis was conducted to measure the influence of the prestressing on changes of eigenfrequencies and eigenmodes. In the second step, a steady dynamic analysis was performed to harmonic excitation to demonstrate the reduction of local amplitudes. Numerical experiments have been conducted on the model of a small rotorcraft. Our results indicate that introduction of initial prestressing may be used to affect natural structure frequencies and to lower the amplitude of vibrations of the structure exposed to external extortions.

**Key words:** prestressing, vibration suppression.

### 1. INTRODUCTION – DYNAMIC RESPONSE STABILISATION AND CHALLENGES IN AEROSPACE ENGINEERING

The problem of dynamic response stabilisation is a crucial issue in many engineering applications. The problem can be addressed to: (a) impact load absorption at the source of this excitation, (b) damping of the impact born, free vibrations or (c) damping of continuously, externally forced vibrations. The first problem in all activities devoted to stabilisation of dynamic response of the structure is identification (usually in real time) of dynamic excitation. It is especially a challenging issue for the impact loads, when in a few milliseconds not only the kinetic energy of the impact but also the impact velocity has to

be determined [1]. Our strategy for impact load absorption will be different for a “slow” impact (high kinetic energy but low velocity) and for a “fast” impact (low kinetic energy but high velocity). Of course, dynamic structural response depends very much on the natural, material damping which can be significantly improved by applying additional passive dampers (e.g. using well selected elastomeric components). In the case of predictable impact loads, various types of passive shock-absorbers can be sufficiently effective (e.g. oil damper and gas spring in a regular landing gear). For predictable externally forced vibrations, magnetorheological [9], tuned inerter dampers [10] and so called tuned mass dampers TMD [13] with properly designed location for extra spring mass can be also effective. However, when the excitation is somehow varied and random [8], the characteristics of our damping device should be adaptable to the identified online load case. We can call this class of shock absorbers AIA (*Adaptive Impact Absorption*). The group of pneumatic/hydraulic flow control shock absorbers with actively controlled piezo valves determines the first class of AIA systems [2], requiring real time feedback control of piezo actuators. The second class is determined by pneumatic systems (e.g. airbags) with controlled special release valves [3]. In this case, less demanding open loop control can be also very effective. The next (semi active) class requires precise on time switching between two active interfaces of adaptive inerter (so called SPINMAN), causing switching of the spin of rotating inertial cylinders for conversion of linear impact energy into rotation of the inerter [4]. Still, semi active AIA systems can be sometimes replaced by passive (simpler, cheaper and lighter), smart solutions and almost equally effective to the first one. Finally, so called PAR (*Prestress Accumulation Release*) adaptive system for damping of impact born vibrations has been demonstrated as an extremely effective algorithm [5, 6].

While concentrating on aerospace engineering, the following requirements are crucial: (a) artificial vibration damping system due to flexibility of the structure and its low natural damping, (b) low weight of the proposed damping system, (c) high reliability (simplicity) of the proposed system. Therefore, semi active (or even smart passive) AIA damping systems will be preferable for aero applications. The concept of predesigned prestressing seems to be one of possible options for aero applications leading to effective reduction of externally forced (impact born or continuously excited) vibrations.

Feasibility study for control of eigen vibrations in flexible truss structures of parabolic mirrors on the orbit, by means of inducing self-stresses has been already performed [7]. It has been demonstrated that ca 15% reduction of local vibration amplitude is available via proper prestressing of the structure. The challenging issue is to find out how far local vibrations (caused by continuous external excitation) with introduced self-stresses (eventually adapting to variable excitation) can be reduced. The second question is how far the effec-

tiveness of the PAR technique described above with initial prestressing can be increased.

The main objective of this paper is to analyse the case study of a rotorcraft with excited high vibrations of the pilot and passenger sites. The effectiveness of eventual reduction of these vibrations by prestressing will give us a good motivation for further research on development of the above mentioned techniques

## 2. BASIC FORMULAS

General equations of motion can be expressed as follows [11]:

$$(2.1) \quad \mathbf{M}\ddot{\mathbf{x}} + \mathbf{C}\dot{\mathbf{x}} + \mathbf{K}\mathbf{x} = \mathbf{F},$$

where  $\mathbf{M}$ ,  $\mathbf{C}$ ,  $\mathbf{K}$  denote the mass, damping and stiffness matrix, respectively. The symbols:  $\ddot{\mathbf{x}}$ ,  $\dot{\mathbf{x}}$ ,  $\mathbf{x}$  denote vectors of space variables (accelerations, velocities and displacements, respectively), while vector  $\mathbf{F}$  denotes external forces. If damping effect and external forces are neglected, the free vibration problem takes the following form:

$$(2.2) \quad \mathbf{M}\ddot{\mathbf{x}} + \mathbf{K}\mathbf{x} = 0$$

and the corresponding solution leads to the formula:

$$(2.3) \quad \mathbf{x} = \boldsymbol{\Phi}e^{j\omega t},$$

where  $\boldsymbol{\Phi}$  denotes the amplitude vector,  $\omega$  denotes the eigenfrequency and  $t$  denotes time. Substitution of the above relation to Eq. (2.2) leads to:

$$(2.4) \quad (\mathbf{K} - \omega^2\mathbf{M})\boldsymbol{\Phi} = 0.$$

We are interested in non-trivial solutions satisfying the following formula:

$$(2.5) \quad \det(\mathbf{K} - \omega^2\mathbf{M}) = 0.$$

Equation (2.5) does not depend on possible initial stresses (so called prestressing: internal, self-equilibrated stresses, caused by geometrical incompatibilities, e.g. thermal distortions). Influence of initial stresses on modal analysis can be taken into account via modification of the stiffness matrix and including additional geometrical stiffness matrix  $\mathbf{K}_G$  [12]. Then, Eq. (2.5) takes its final form:

$$(2.6) \quad \det(\mathbf{K} + \mathbf{K}_G - \omega^2\mathbf{M}) = 0.$$

In commercial FEM systems, like Abaqus, the modal analysis of prestressed structures is performed in two steps. In the first step, the static analysis  $\mathbf{K}\mathbf{x} = \mathbf{F}$

defined for nonlinear geometry has to be solved. Then, the determined solution allows calculation of the geometric stiffness matrix  $\mathbf{K}_G$  and modification of the stiffness matrix  $\mathbf{K}$  (cf. Eq. (2.6)) in the second step, leading to the final modal analysis.

Prestressing causes modification of both eigenfrequencies and eigenmodes. The MAC (Modal Assurance Criterion) [14] coefficient has been used as a measure of correlation between two eigenmodes of vibration

$$(2.7) \quad \text{MAC} = \frac{|\boldsymbol{\Phi}_R^T \boldsymbol{\Phi}_M|^2}{(\boldsymbol{\Phi}_R^T \boldsymbol{\Phi}_M)(\boldsymbol{\Phi}_R^T \boldsymbol{\Phi}_M)},$$

where  $\boldsymbol{\Phi}_R$  is the vector of reference eigenmode of vibration,  $\boldsymbol{\Phi}_M$  is the vector of eigenmode of vibration for prestressed structure.

### 3. NUMERICAL EXPERIMENTS ON THE MODEL OF SMALL ROTORCRAFT

Numerical model of small rotorcraft, based on the construction of a real light rotorcraft has been elaborated taking advantage of the Abaqus program. The FEM model (Fig. 1) consisting of 69366 shell elements (S4, S4R, S3, S3R) and 394 beam elements (B31) allows relatively good representation of the real structure geometry. We have used fully integrated elements S3 and S4 to model properties of shells (e.g. internal walls, floors, cabin), while elements with reduced integration (S3R, S4R, B31) have been used to model properties of additional elements (e.g. tubular landing skids, main transmission and engine mountings) which have small influence on the investigated part of the model. We have also used commonly known material data of materials like steel and aluminium alloys. Major substructures, such as engine and main gear, have been modelled

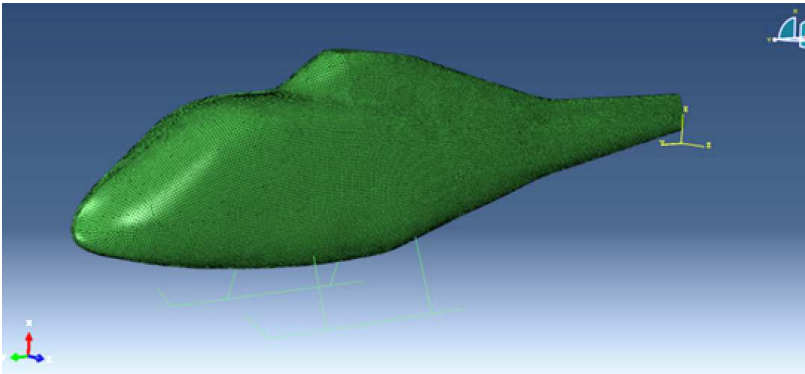


FIG. 1. General view of numerical model of the selected small rotorcraft.

as rigid parts with mass distribution taken from official industrial catalogues. Other equipment of the rotorcraft (e.g. pilot seats) has been modelled in an approximate way, with the use of geometric figures. The boundary conditions have been defined by fixing four supporting points on the landing gear (in three orthogonal directions).

The main goal of our case study is the numerical experiment evaluating feasibility of reduction (by prestressing) of vertical vibration amplitude (critical frequency range 22–25 Hz correlated with the rotor operational frequency) for the rotorcraft floor in the passenger section.

Let us analyse the effectiveness of prestressing by sticking (e.g. gluing) initially extended metal strips into the floor just below passenger seats (Fig. 2). Six 60 mm wide strips with 85 mm gaps between them and with various geometrical incompatibility (prestress force) have been tested. At this stage of investigations we have assumed that metal strips are made of material with steel properties and without yield strength. Although prestress force, as it is shown further, causes a high level of stress, lately in the aircraft industry materials with ultra high strength yield e.g. Ferrium S53, 300M, 4340 (with strength yield above 1500 MPa) have been commonly used. For example, S53 steel is being used in some demanding landing gear and helicopter rotor shaft applications.

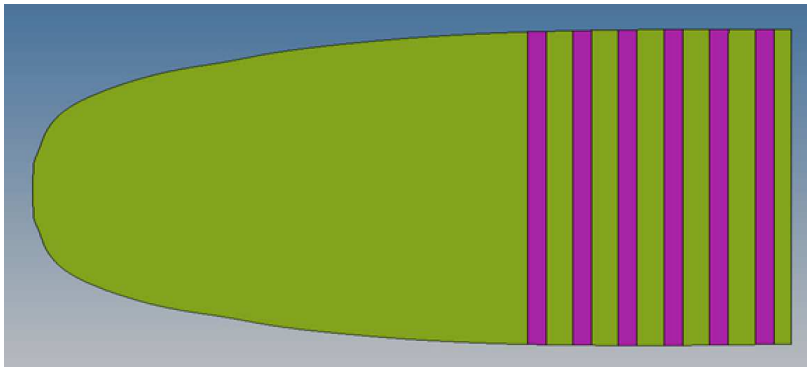


FIG. 2. Distribution of prestressing strips on the cabin floor.

The sequence of numerical tests of dynamic response performed for harmonic, kinematic excitation applied to main gear of the rotorcraft is the following:

- The first step was modal analysis of the rotorcraft model without introduced prestress, in order to generate the reference response. Critical frequencies and localisation of maximum vibration amplitudes (passenger seats) have been determined.

- The second step was devoted to **modifications of modal response** for prestressed structure and was divided into two substeps:
  - application of prestressing elements (sticked, extended strips) on the floor allowing generation of properly tuned initial stresses in the structure,
  - modal analysis of prestressed structure in order to generate expected dynamic response for further comparison with reference response (eigenfrequencies shift and MAC correlation index for eigenmodes).
- The third step is devoted to demonstration of **reduction for local amplitudes** (of vibration) in vicinity of passenger seats.

#### 4. MODIFICATION OF MODAL RESPONSE DUE TO PRESTRESSING

On the base of the first step, eigenfrequencies and eigenmodes in the range of 0–30 Hz have been determined identifying 20 vibration modes. The low frequency modes (2.7–14.0 Hz) correspond to global vibrations (vertical and horizontal) of the entire structure. Higher frequencies (17–28 Hz) correspond mainly to vibrations of elements from the pilot and passenger compartments. Frequencies 20–30 Hz correspond also to vibrations of the propulsion system and vibrations of diaphragms dividing separate sections of the rotorcraft.

The eigenfrequency 24.08 Hz has been selected for further analysis (on the basis of the second step of analysis) as the most critical. The mode shape associated with the 14th natural frequency is shown in Fig. 3a. The corresponding high amplitudes of vibrations for the passenger seats cause a significant biotechnical problem.

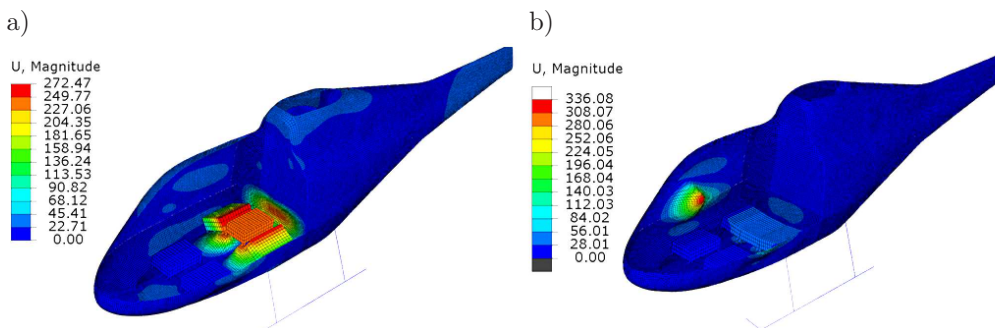


FIG. 3. Mode shape associated with the 14th natural frequency: a) basic structure, b) prestressed structure.

Depending on the generated prestress level, the eigenfrequency for the 14th eigenmode modifies its value (Fig. 4). One can observe shift of the eigenfrequency up to above 13%.

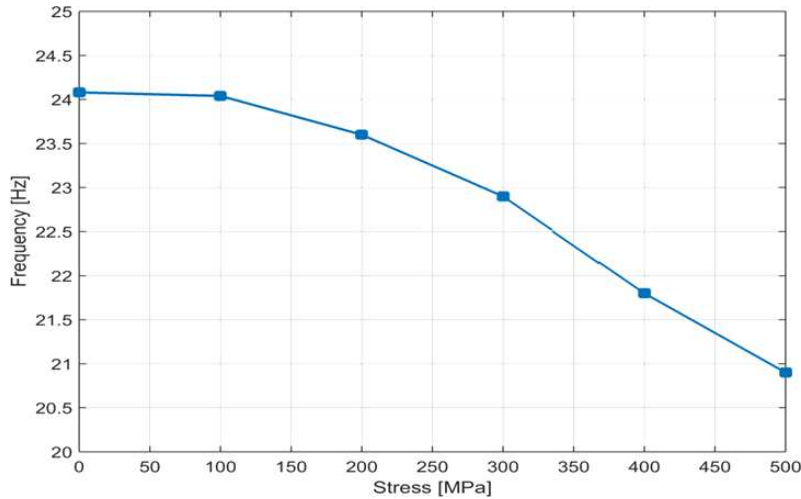


FIG. 4. 14th eigenfrequency vs generated initial stresses.

Modifications of the 14th eigenmode parameters due to generation of the initial stresses equal to 500 MPa are presented in Table 1 and shown in Fig. 3b.

Table 1. Result summary.

Eigenfrequency for reference structure [Hz]	Prestressed structure		MAC coefficient
	Eigenfrequency [Hz]	Modification [%]	
24.08	20.86	13.33	0.6

5. REDUCTION OF LOCAL AMPLITUDES OF VIBRATION DUE TO PRESTRESSING

The 3rd step analysis has been performed on the basis of the Abaqus program with “direct steady state dynamic” analysis that allows to determine structural steady state response for harmonic excitation. In principle, this approach is linear but it allows taking into account nonlinearities, e.g. geometrical, defined in previous time steps. That is why the static analysis with geometric nonlinearities included has been applied prior to the approach described above, which allows introducing initial stresses in selected elements. First, the equilibrium forces between the structural part with imposed incompatible distortions (generating finally self-equilibrated state of initial stresses) and the remaining structural part have to be determined. Further modal analysis is performed for the structure with self-stresses involved. The same prestressing operation has been applied as in the previous section (Fig. 2).

It has been assumed that the dominating, external, harmonic excitations are generated by the rotor, operating above the cabin roof. The rotor, composed of

three blades, is rotating with the nominal angular velocity of 440 cycles/min. The blades passing above the cabin roof are exposed to increased aerodynamic pressure transmitted along the rotor. It can generate ca  $3 \times 440 = 1320$  impulses per minute. It corresponds to the frequency 22 Hz of harmonic excitation applied to our rotorcraft. If producer allows increment of rotor operational frequency up to 115% of the nominal frequency, it corresponds to the increase of external harmonic excitation applied to the structure up to 25 Hz. In consequence, the 3rd step of analysis has been focused on external excitations in the range of 20–26 Hz (overlapping range 22–25 Hz of expected frequencies coming from the operating rotor).

The analysed critical range of excitations (20–26 Hz) has been divided into 26 intervals and kinematic excitation with the amplitude of 1 mm has been applied (each time) to the main gear element. Note that the eigenfrequency 24.08 Hz of the basic structure (without prestress) analysed in steps 1 and 2 is included into the range of excitations analysed in step 3.

Dynamic structural response for two external excitations: 23.91 and 24.41 Hz (close to the eigenfrequency of the basic model) are shown in Figs. 5 and 6. Large

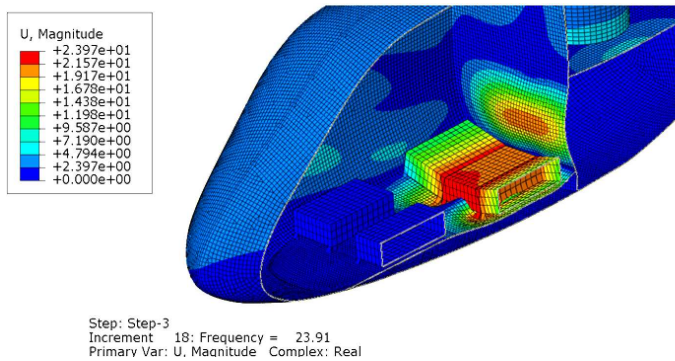


FIG. 5. Dynamic response for harmonic excitation 23.91 Hz (basic structure).

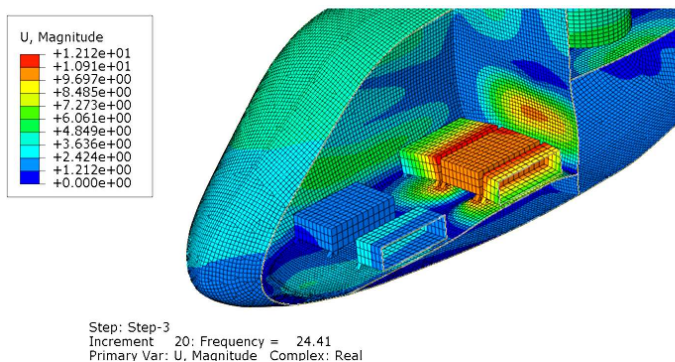


FIG. 6. Dynamic response for harmonic excitation 24.41 Hz (basic structure).

vibration amplitudes of the passenger seats and the neighboring internal parts of the structure can be observed.

Displacements of the passenger seat surfaces (in the cross-section orthogonal to the longitudinal direction of the rotorcraft, normalised to the cabin width) are shown in Fig. 7. A simplistic way of seats' modelling cause kinks observed in Fig. 7a. Displacements of the floor just below these seats are shown in Fig. 7b. Reduction of amplitude observed in the central part of Fig. 7b is caused by the structural reinforcement located along the central axis of the cabin floor.

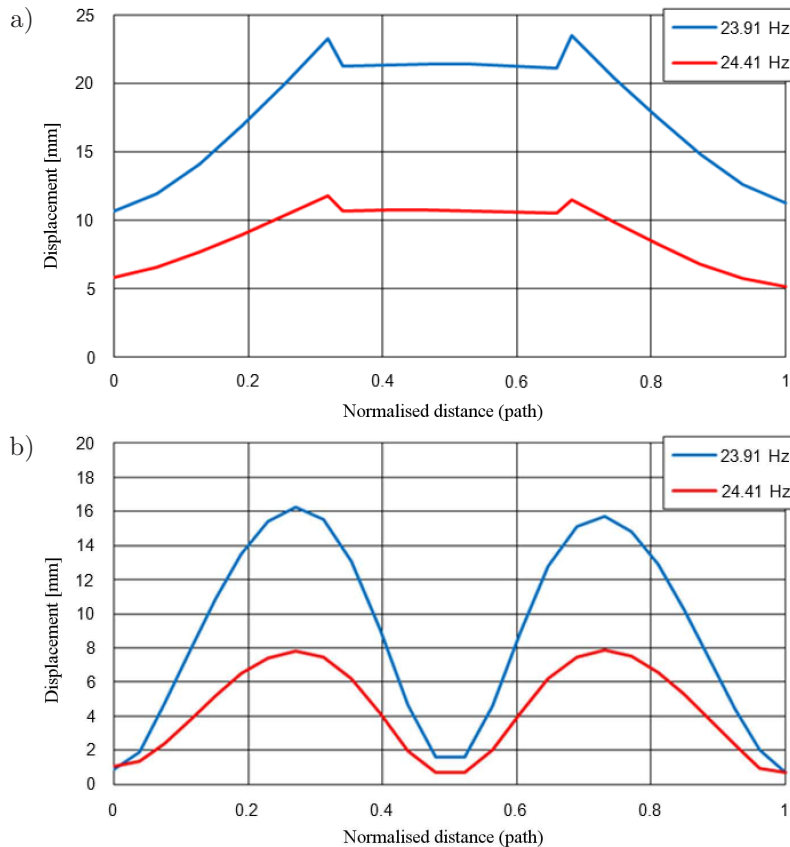


FIG. 7. Displacements along: a) the surface of passenger's seat, b) the floor under the passenger's seat for harmonic excitation 23.91 Hz and 24.41 Hz (basic structure).

Displacements of a selected node of the passenger's seat versus frequencies of externally forced harmonic excitations are shown in Fig. 8. Large displacements in the range of 22–25 Hz can be observed.

Analogous analysis (to the described above) has been performed for the prestressed structure (with the same technique for generation of initial stresses as in

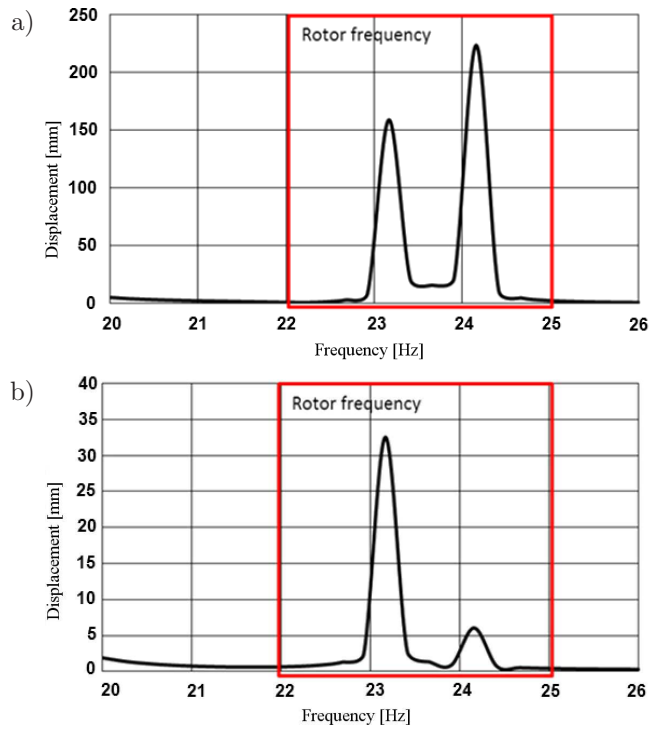


FIG. 8. Displacements of: a) the middle seat, b) the floor below the middle seat versus excited frequencies (basic structure, harmonic excitation).

step 2). The dynamic structural responses for the external harmonic excitations (23.91 Hz and 24.41 Hz) are shown in Figs. 9 and 10, where significant reduction (up to ca 33%) of vibration amplitudes of the floor below the passenger seats can be observed. However, significant, corresponding increase of vibration amplitudes in lateral walls of the cabin is also registered.

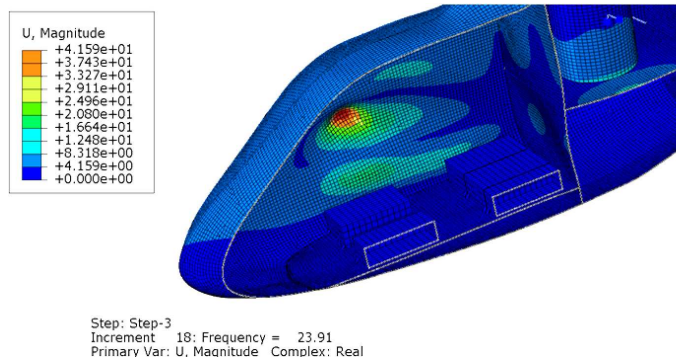


FIG. 9. Dynamic response for harmonic excitation 23.91 Hz (prestressed structure).

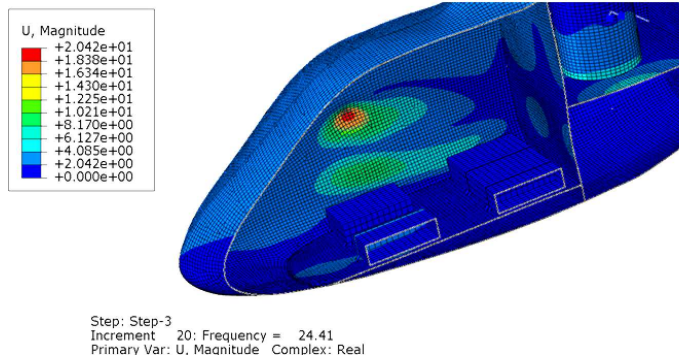


FIG. 10. Dynamic response for harmonic excitation 24.41 Hz (prestressed structure).

Displacements of the passenger seat surfaces (in the cross-section orthogonal to the longitudinal direction of the rotorcraft, normalised to the cabin width) are shown in Fig. 11a for the prestressed structure. Dramatic reduction of am-

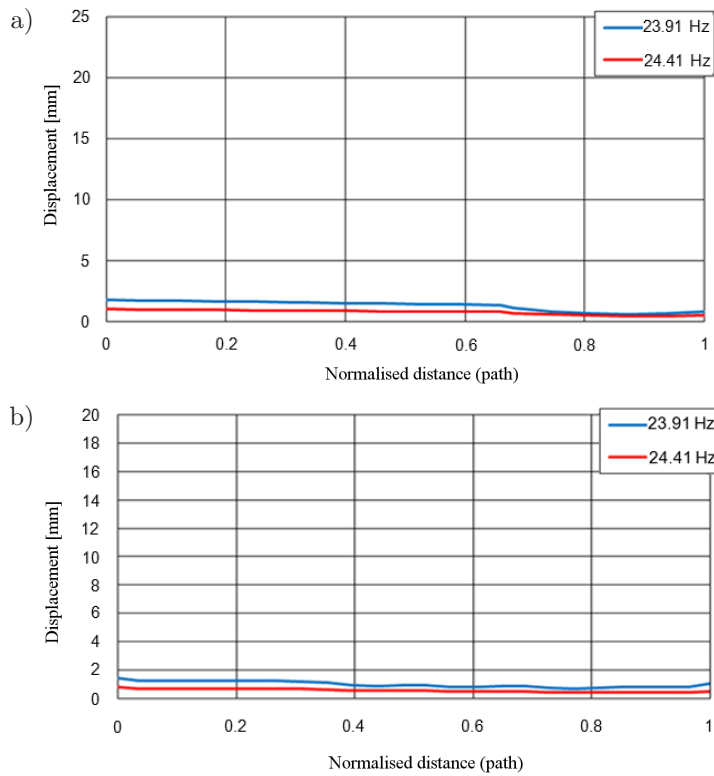


FIG. 11. Displacements along: a) the surface of passenger’s seat, b) the floor under the passenger’s seat for harmonic excitation 23.91 Hz and 24.41 Hz (prestressed structure, harmonic excitation).

plitudes (ca 10 times) in comparison to the amplitudes for the basic structure (Fig. 7a) can be observed. Also, displacements of the floor just below these seats (for prestressed structure) are shown in Fig. 11b. Reduction of amplitude due to prestressing is also dramatic (8 times for the excitation 24.41 Hz and 16 times for the excitation 23.91 Hz – cf. Fig. 7b).

Displacements of a selected node of the passenger seat versus frequencies of externally forced harmonic excitations (for the prestressed structure) are shown in Fig. 12a, where dramatic reductions of amplitudes (for the frequencies 24.1 and 23.1 Hz) compared with amplitudes for the basic structure (Fig. 8) can be observed. Only one pick of amplitude (in the range of 22–25 Hz), much smaller than for the basic structure, is registered. Similar results can be observed for displacements measured on the floor below the passenger seats (Fig. 12b).

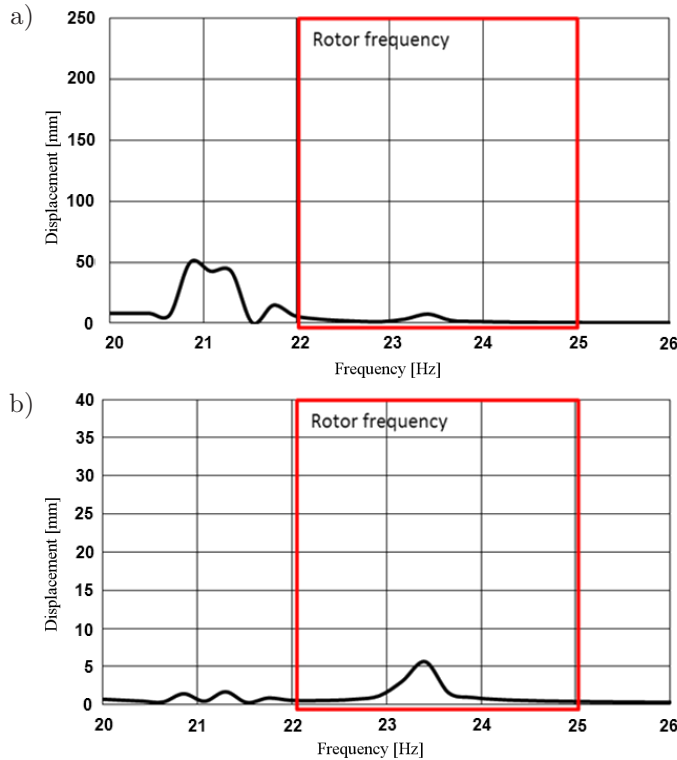


FIG. 12. Displacements of: a) the middle seat, b) the floor below the middle seat versus excited frequencies (compressed structure, harmonic excitation).

## 6. CONCLUSIONS

The analysed case study shows that over 13% shifting of the structural eigenfrequency (and the corresponding 40% reduction of the MAC index) is achievable

via introducing of prestress. It has been also demonstrated that properly tuned initial stresses induced in the structure via initial distortions (incompatibilities) forced in one location can reduce vibration amplitudes in another, selected (crucial) location very effectively. However, the side effect of such an operation can be an increase of vibration amplitudes in another location on the structure. One can say that the prestressing technique can be very effective in local isolation of structural vibration amplitudes caused by some critical external excitation. An important advantage of the proposed technique, especially for aeronautic and aerospace applications, is a new option for reducing unwanted vibrations without increasing the structural mass.

The magnitude of modification of the dynamic, structural response depends on overall structural stiffness and sensitivity of defined objective function for admissible structural modifications in selected localisations. The above results motivate authors for further, more methodological studies on control of structural dynamic response based on modifiable prestressing technique, which will be published in a separate paper. The challenges to overcome require inclusion of the material damping effect, which will make the computational task more hard, but will also lead to more realistic results. Also, the problem of prestress optimisation (location for generation of prestress distortions and their magnitude) and technologies for prestress inducing (preferable in a modifiable manner) are open questions.

#### ACKNOWLEDGMENT

Financial support of the National Science Centre, Poland, granted through the projects “Ad-DAMP” (DEC-2014/15/B/ST8/04363) and “AIA” (DEC-2012/05/B/ST8/02971), is gratefully acknowledged.

#### REFERENCES

1. SEKUŁA K., GRACZYKOWSKI C., HOLNICKI-SZULC J., *On-line impact load identification*, Shock and Vibration, **20**(1): 123–141, 2013.
2. MIKUŁOWSKI G., WISZOWATY R., HOLNICKI-SZULC J., *Characterization of a piezoelectric valve for an adaptive pneumatic shock absorber*, Smart Materials and Structures, **22**(12): 125011-1-12, 2013.
3. GRACZYKOWSKI C., HOLNICKI-SZULC J., *Protecting offshore wind turbines against ship impacts by means of Adaptive Inflatable Structures*, Shock and Vibration, **16**(4): 335–353, 2009.
4. FARAJ R., HOLNICKI-SZULC J., KNAP L., SEŃKO J., *Adaptive inertial shock-absorber*, Smart Materials and Structures, **25**(3): 035031-1-9, 2016.

5. MRÓZ A., ORŁOWSKA A., HOLNICKI-SZULC J., *Semi-active damping of vibrations, Prestress Accumulation-Release strategy development*, Shock and Vibration, **17**(2): 123–136, 2010.
6. MRÓZ A., HOLNICKI-SZULC J., BICZYK J., *Prestress Accumulation-release technique for damping of impact-born vibrations: application to self-deployable structures*, Mathematical Problems in Engineering, **2015**: 720236-1-9, 2015.
7. HOLNICKI-SZULC J., HAFTKA R., *Vibration mode shape control by prestressing*, AIAA Journal, **30**(7): 1924–1927, 1992.
8. RADKOWSKI S., SZULIM P., *Analysis of vibration of rotors in unmanned aircraft*, 19th International Conference on Methods and Models in Automation and Robotics (MMAR), pp. 748–753, Międzyzdroje, Poland, September, 2–5, 2014.
9. BAJKOWSKI J., JASIŃSKI M., MAĆZAK J., RADKOWSKI S., ZALEWSKI R., *The active magnetorheological support as an element of damping of vibrations transferred from the ground to large-scale structure supports*, Key Engineering Materials, **518**: 350–357, 2012.
10. LAZAR I.F., NEILD S.A., WAGG D.J., *Using an inerter-based device for structural vibration suppression*, Earthquake Engineering and Structural Dynamics, **43**(8): 1129–1147, 2014.
11. HUMAR J.L., *Dynamics of structures*, CRC Press, Boca Raton, London, New York, Leiden, 2002.
12. BEDRI R., AL-NAIS M.O., *Prestressed modal analysis using finite element package ANSYS*, Lecture Notes in Computer Science vol. 3401, pp. 171–178, 2005. ([in:] Numerical Analysis and Its Applications: 3rd International Conference, NAA 2004, Rousse, Bulgaria, June 29–July 3, 2004, Springer, Berlin, Heidelberg, pp. 171–178, ISBN 978-3-540-31852-1).
13. RANA R., SONG T.T., *Parametric study and simplified design of tuned mass dampers*, Engineering Structures, **20**(3): 193–204, 1998.
14. ALLEMANG R.J., *The modal assurance criterion (MAC): twenty years of use and abuse*, Proceedings of IMAC 20, The International Modal Analysis Conference, Los Angeles, CA, USA, pp. 397–405, 2002.

*Received April 5, 2016; accepted version June 30, 2016.*

---